

ELASTIC REDATUMING OF MULTICOMPONENT SEISMIC DATA¹

C. P. A. WAPENAAR,² H. L. H. COX³ and A. J. BERKHOUT²

ABSTRACT

WAPENAAR, C.P.A., COX, H.L.H. and BERKHOUT, A.J. 1992. Elastic redatuming of multi-component seismic data. *Geophysical Prospecting* **40**, 465–482.

Elastic redatuming can be carried out before or after decomposition of the multi-component data into independent PP, PS, SP, and SS responses. We argue that from a practical point of view, elastic redatuming is preferably applied after decomposition. We review forward and inverse extrapolation of decomposed P- and S-wavefields. We use the forward extrapolation operators to derive a model of discrete multicomponent seismic data. This forward model is fully described in terms of matrix manipulations.

By applying these matrix manipulations in reverse order we arrive at an elastic processing scheme for multicomponent data in which elastic redatuming plays an essential role. Finally, we illustrate elastic redatuming with a controlled 2D example, consisting of simulated multicomponent seismic data.

INTRODUCTION

Seismic redatuming is a popular concept, indicating the wave field extrapolation process that transforms seismic measurements from the actual data acquisition surface (old datum) to a simulated data acquisition surface (new datum) further down in the subsurface. Often the new datum will present the top of a target zone. After redatuming the propagation effects (down and up) of the target overburden have been removed from the target reflections and, particularly for a structurally complicated overburden, the target response will be simplified significantly. An important practical aspect of redatuming is that the macromodel of the subsurface should be known.

Prestack redatuming was applied by Berryhill (1984) for the 2D acoustic situation and modified by Kinneging *et al.* (1989) for the 3D acoustic situation. We discuss an elastic redatuming scheme for multicomponent seismic data. The theory

¹ Presented at the 52nd EAEG meeting, Copenhagen, May–June 1990; received August 1990, revision accepted December 1991.

² Delft University of Technology, P.O. Box 5046, 2600 GA Delft, The Netherlands.

³ Geco-Prakla Delft, P.O. Box 148, 2600 AC Delft, The Netherlands.

is presented for the 3D inhomogeneous anisotropic situation and is illustrated with a redatuming example for a 2D inhomogeneous isotropic elastic medium. In order to perform elastic redatuming the macro-models for both P- and S-waves should be known. Any inconsistency between the two macromodels may have serious consequences for the subsequent inversion step(s).

REDATUMING BEFORE OR AFTER DECOMPOSITION?

Redatuming is ideally based on non-recursive wavefield extrapolation from the acquisition surface to the top level of a target zone. In the acoustic version, the wavefield extrapolation operators are derived from the acoustic Kirchhoff-Helmholtz (KH) integral. Therefore, for the elastic version it seems natural to derive the wavefield extrapolation operators directly from the elastic KH integral. Consider the frequency-domain representation of the integral

$$u_m(\mathbf{r}_A, \omega) = \iint_{-\infty}^{\infty} [\boldsymbol{\theta}_m(\mathbf{r}, \mathbf{r}_A, \omega) \cdot \mathbf{u}(\mathbf{r}, \omega) - \mathbf{g}_m(\mathbf{r}, \mathbf{r}_A, \omega) \cdot \boldsymbol{\tau}(\mathbf{r}, \omega)]_{z_0} dx dy \quad (1)$$

(De Hoop 1958; Burridge and Knopoff 1964; Aki and Richards 1980; Wapenaar and Berkhout 1989). Here $\mathbf{u}(\mathbf{r}, \omega)$ and $\boldsymbol{\tau}(\mathbf{r}, \omega)$ represent the elastic wavefield in terms of the space [$\mathbf{r} = (x, y, z)$] and frequency (ω) dependent displacement (\mathbf{u}) and traction ($\boldsymbol{\tau}$), respectively. Similarly, $\mathbf{g}_m(\mathbf{r}, \mathbf{r}_A, \omega)$ and $\boldsymbol{\theta}_m(\mathbf{r}, \mathbf{r}_A, \omega)$ represent a Green's wavefield in terms of the space and frequency-dependent Green's displacement (\mathbf{g}_m) and Green's traction ($\boldsymbol{\theta}_m$), respectively. The Green's wavefield is an elastic wavefield that would be present when an impulsive unit body force were placed at $\mathbf{r}_A = (x_A, y_A, z_A)$. The subscript m refers to the direction of this body force: for $m = x, y$ or z , the force acts in the x -, y - or z -direction, respectively. Hence, (1) states that the m -component (i.e. the x -, y - or z -component) of the displacement vector \mathbf{u} at \mathbf{r}_A can be computed from the displacement and traction distribution at $z = z_0$, see Fig. 1. Equation (1) is exact for any source-free inhomogeneous anisotropic lower half-space $z > z_0$. In general, however, no analytical expressions are available for the Green's wave field ($\mathbf{g}_m, \boldsymbol{\theta}_m$). So in practice the Green's wavefield at $z = z_0$ should be computed by numerically modelling the response of an impulsive unit body force at \mathbf{r}_A . To this end, one should have available a model of the half-space $z > z_0$ in terms of the space-dependent mass density $\rho(\mathbf{r})$ and the stiffness tensor $c_{ijkl}(\mathbf{r})$ for the anisotropic situation, or the P- and S-wave velocities $c_p(\mathbf{r})$ and $c_s(\mathbf{r})$ for the isotropic

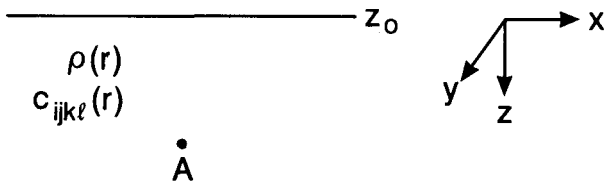


FIG. 1. Configuration for the Kirchhoff-Helmholtz integral (1). The elastic lower half-space $z > z_0$ may be arbitrarily inhomogeneous and anisotropic and is assumed to be source-free.

situation. Fortunately, for the purpose of wave-field extrapolation, a geologically oriented macromodel of these parameters will suffice (Berkhout 1986). This means that redatuming (acoustic or elastic) should always be preceded by macromodel estimation. A discussion of macromodel estimation is beyond the scope of this paper; we refer the reader to Faye and Jeannot (1986) and Cox *et al.* (1988). Any estimated macromodel contains some errors. For the acoustic case, experience has shown that small errors in the macromodel (typically 5%) are not disastrous for wavefield extrapolation: the only effect is some defocusing and mispositioning of seismic events. For the elastic case, however, the situation is more complicated since two macromodels are involved. To illustrate this important property, consider (1) and bear in mind that the elastic wavefield (\mathbf{u} , $\boldsymbol{\tau}$) as well as the Green's wavefield (\mathbf{g}_m , $\boldsymbol{\theta}_m$) are composed of (quasi) P- and S-wave contributions:

$$\mathbf{u}(\mathbf{r}, \omega) = \mathbf{u}^P(\mathbf{r}, \omega) + \mathbf{u}^S(\mathbf{r}, \omega), \quad (2a)$$

$$\boldsymbol{\tau}(\mathbf{r}, \omega) = \boldsymbol{\tau}^P(\mathbf{r}, \omega) + \boldsymbol{\tau}^S(\mathbf{r}, \omega), \quad (2b)$$

$$\mathbf{g}_m(\mathbf{r}, \mathbf{r}_A, \omega) = \mathbf{g}_m^P(\mathbf{r}, \mathbf{r}_A, \omega) + \mathbf{g}_m^S(\mathbf{r}, \mathbf{r}_A, \omega) \quad (2c)$$

and

$$\boldsymbol{\theta}_m(\mathbf{r}, \mathbf{r}_A, \omega) = \boldsymbol{\theta}_m^P(\mathbf{r}, \mathbf{r}_A, \omega) + \boldsymbol{\theta}_m^S(\mathbf{r}, \mathbf{r}_A, \omega). \quad (2d)$$

Hence, for the dot products $\boldsymbol{\theta}_m \cdot \mathbf{u}$ and $\mathbf{g}_m \cdot \boldsymbol{\tau}$ we may write

$$\boldsymbol{\theta}_m \cdot \mathbf{u} = \boldsymbol{\theta}_m^P \cdot \mathbf{u}^P + \boldsymbol{\theta}_m^P \cdot \mathbf{u}^S + \boldsymbol{\theta}_m^S \cdot \mathbf{u}^P + \boldsymbol{\theta}_m^S \cdot \mathbf{u}^S \quad (3a)$$

and

$$\mathbf{g}_m \boldsymbol{\tau} = \mathbf{g}_m^P \cdot \boldsymbol{\tau}^P + \mathbf{g}_m^P \cdot \boldsymbol{\tau}^S + \mathbf{g}_m^S \cdot \boldsymbol{\tau}^P + \mathbf{g}_m^S \cdot \boldsymbol{\tau}^S \quad (3b)$$

Here \mathbf{g}_m^P and $\boldsymbol{\theta}_m^P$ are largely determined by the macromodel for the P-wave velocity $c_p(\mathbf{r})$, whereas \mathbf{g}_m^S and $\boldsymbol{\theta}_m^S$ are largely determined by the macromodel for the S-wave velocity $c_s(\mathbf{r})$. Hence, in (3a) and (3b) different terms that depend on different macromodels are superposed. This is prescribed by the theory, and (1) yields the correct displacement $u_m(\mathbf{r}_A, \omega)$ when both macromodels are correct. However, when the P- and S-wave macromodels are only slightly erroneous, (3a) and (3b) may easily lead to an 'out-of-phase' superposition of the different terms, thus introducing artifacts. (These artifacts cannot be removed by applying decomposition at the new datum afterwards).

This observation does not only apply to elastic redatuming but to any elastic migration or inversion scheme that operates directly on the multicomponent data rather than on decomposed data.

As an alternative, consider the following expressions for extrapolation of decomposed wavefields:

$$\begin{aligned} \phi(\mathbf{r}_A, \omega) = & \iint_{-\infty}^{\infty} \frac{2}{\rho\omega^2} \\ & \times \left[\frac{\partial \gamma_{\phi}^{\bar{}} \phi(\mathbf{r}, \mathbf{r}_A, \omega)}{\partial z} \phi^+(\mathbf{r}, \omega) + \frac{\partial \gamma_{\psi}^{\bar{}} \phi(\mathbf{r}, \mathbf{r}_A, \omega)}{\partial z} \cdot \psi^+(\mathbf{r}, \omega) \right]_{z_0} dx dy \quad (4a) \end{aligned}$$

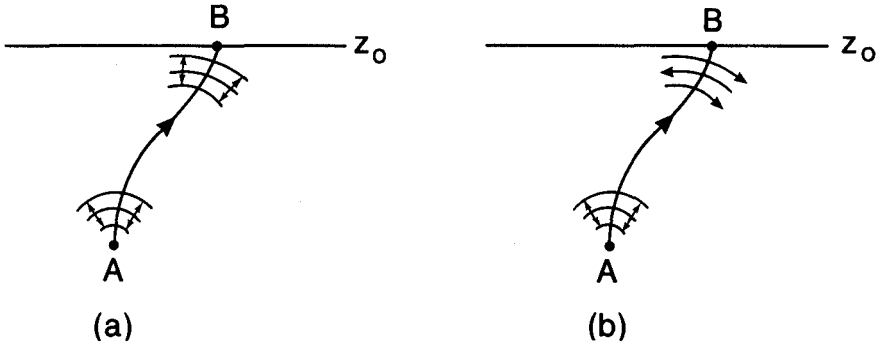


FIG. 2. Green's wavefields related to a P-wave source. (a) Green's P-wave potential $\gamma_{\phi, \phi}^-(\mathbf{r}_B, \mathbf{r}_A, \omega)$; (b) Green's S_y -wave potential $\gamma_{\psi_y, \phi}^-(\mathbf{r}_B, \mathbf{r}_A, \omega)$, being the y -component of $\gamma_{\psi, \phi}^-(\mathbf{r}_B, \mathbf{r}_A, \omega)$.

and

$$\psi_h(\mathbf{r}_A, \omega) = \iint_{-\infty}^{\infty} \frac{2}{\rho \omega^2} \times \left[\frac{\partial \gamma_{\phi, \psi_h}^-(\mathbf{r}, \mathbf{r}_A, \omega)}{\partial z} \phi^+(\mathbf{r}, \omega) + \frac{\partial \gamma_{\psi, \psi_h}^-(\mathbf{r}, \mathbf{r}_A, \omega)}{\partial z} \cdot \Psi^+(\mathbf{r}, \omega) \right] dx dy \quad (4b)$$

(Wapenaar and Haimé 1990, hereafter referred to as paper I). Here $\phi^+(\mathbf{r}, \omega)$ and $\Psi^+(\mathbf{r}, \omega)$ represent the downgoing elastic wavefield at \mathbf{r} in terms of P- and S-wave potentials respectively. Similarly, $\gamma_{\phi, \phi}^-(\mathbf{r}, \mathbf{r}_A, \omega)$ and $\gamma_{\psi, \phi}^-(\mathbf{r}, \mathbf{r}_A, \omega)$ represent the upgoing Green's wavefield at \mathbf{r} in terms of Green's P- and S-wave potentials respectively, related to an impulsive unit P-wave source at \mathbf{r}_A (Fig. 2). Finally, $\gamma_{\phi, \psi_h}^-(\mathbf{r}, \mathbf{r}_A, \omega)$ and $\gamma_{\psi, \psi_h}^-(\mathbf{r}, \mathbf{r}_A, \omega)$ represent the upgoing Green's wavefield at \mathbf{r} in terms of Green's P- and S-wave potentials respectively, related to an impulsive S_h -wave source at \mathbf{r}_A (Fig. 3) (an S_h -wave ($h = x, y$ or z) is an S-wave, polarized in the plane

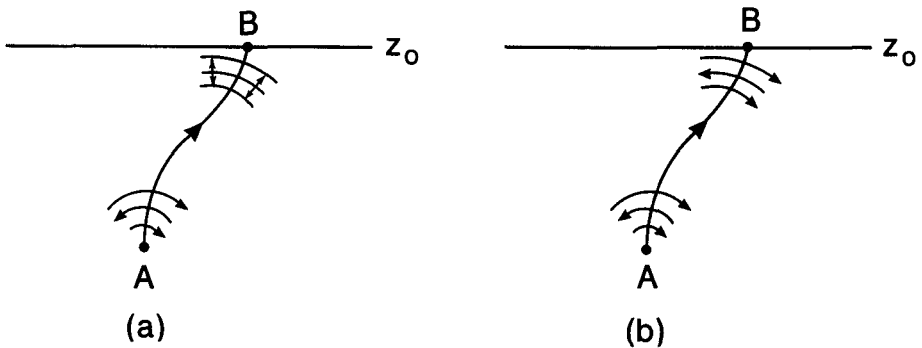


FIG. 3. Green's wavefields related to an S_y -wave source. (a) Green's P-wave potential $\gamma_{\phi, \psi_y}^-(\mathbf{r}_B, \mathbf{r}_A, \omega)$; (b) Green's S_y -wave potential $\gamma_{\psi_y, \psi_y}^-(\mathbf{r}_B, \mathbf{r}_A, \omega)$, being the y -component of $\gamma_{\psi, \psi_y}^-(\mathbf{r}_B, \mathbf{r}_A, \omega)$.

perpendicular to the x -, y - or z -axis). Equations (4a) and (4b) state that the P-wave potential ϕ and the S_h -wave potential ψ_h respectively at \mathbf{r}_A can be computed from the P- and S-wave potentials at $z = z_0$. Equations (4a) and (4b) are exact for any source-free inhomogeneous anisotropic lower half-space $z > z_0$; the only assumption is that the medium is locally homogeneous and isotropic at $z = z_0$ and $\mathbf{r} = \mathbf{r}_A$ (see paper I).

Again in practice the Green's potentials should be computed by numerical modelling and again, in general the expressions are very sensitive to inconsistencies in the P- and S-wave macromodels. Let us now assume that ϕ^+ and Ψ^+ in (4a) represent the decomposed elastic wavefield related to a P-wave source. Then the second term under the integral is a product of converted waves and thus may be ignored. Hence, in this situation (4a) can be approximated by

$$\phi(\mathbf{r}_A, \omega) \approx \iint_{-\infty}^{\infty} \left[\frac{2}{\rho\omega^2} \frac{\partial \gamma_{\phi, \phi}^-(\mathbf{r}, \mathbf{r}_A, \omega)}{\partial z} \phi^+(\mathbf{r}, \omega) \right]_{z_0} dx dy. \quad (5a)$$

Similar arguments lead to the conclusion that for an elastic wavefield related to an S-wave source (4b) can be approximated by

$$\psi_h(\mathbf{r}_A, \omega) \approx \iint_{-\infty}^{\infty} \left[\frac{2}{\rho\omega^2} \frac{\partial \gamma_{\psi_h, \psi_h}^-(\mathbf{r}, \mathbf{r}_A, \omega)}{\partial z} \cdot \Psi^+(\mathbf{r}, \omega) \right]_{z_0} dx dy. \quad (5b)$$

Equations (5a) and (5b) describe *independent* extrapolation of P- and S-waves. Application of (5a) requires knowledge of the P-wave macromodel whereas application of (5b) requires knowledge of the S-wave macromodel. After wavefield decomposition, these macromodels can be estimated independently from the P-P and S-S data, respectively. The accuracy requirements are much less restrictive than for multicomponent wavefield extrapolation, as described by (1). Since (5a) is fully equivalent to the Rayleigh II integral for acoustic wavefield extrapolation (Berkhout 1985), the P-wave macromodel need not be more accurate than the macromodel for acoustic wavefield extrapolation. For the anisotropic situation, the S-wave macromodel needs additional discussion. From (5b) it follows that all components of $\Psi^+(\mathbf{r}, \omega)$ at z_0 contribute to $\psi_h(\mathbf{r}_A, \omega)$, hence (5b) fully accounts for shear-wave splitting. So actually two S-wave macromodels are required, for the slow and fast S-waves respectively. From here onwards we assume that the main form of anisotropy is azimuthal anisotropy with the principal axes (x' , y') making a constant angle θ with the x - and y -coordinate axes. Ignoring shear wave splitting in the natural coordinate system (x' , y' , z) of the anisotropic medium, (5b) may be further approximated by

$$\hat{\psi}_h(\mathbf{r}_A, \omega) \approx \iint_{-\infty}^{\infty} \left[\frac{2}{\rho\omega^2} \frac{\partial \hat{\gamma}_{\psi_h, \psi_h}^-(\mathbf{r}, \mathbf{r}_A, \omega)}{\partial z} \hat{\psi}_h^+(\mathbf{r}, \omega) \right]_{z_0} dx dy, \quad (5c)$$

for $h = x'$ or y' , where $\hat{\psi}_h^+$ and $\hat{\gamma}_{\psi_h, \psi_h}^-$ represent the h -component of Ψ^+ and $\hat{\gamma}_{\psi_h, \psi_h}^-$ respectively, the hats ($\hat{\quad}$) referring to the natural coordinate system. Equation (5c) for $h = x'$ and y' describes *independent* extrapolation of the slow and fast S-waves. Since this decoupled equation is fully equivalent to the acoustic Rayleigh II integral, the slow and fast S-wave macromodels also need not be more accurate than an acoustic model. In the following the primes ($'$) will be omitted for notational convenience.

To summarize: in theory elastic redatuming can either be based on the two-way KH integral (1) or on the one-way Rayleigh integrals (5a) and (5c). Equation (1) is exact, but it requires an unrealistically accurate macro-model. On the other hand, (5a) and (5c) ignore second-order contributions, but they are not more sensitive to macromodel errors than the acoustic Rayleigh integral. Hence, from a practical point of view the one-way approach is preferable.

In analogy with Berkhout and Wapenaar (1988), we propose the following processing sequence for elastic redatuming:

1. Decomposition at the surface of the multicomponent data into P-P, P-S, S-P and S-S data.
2. Elimination of the surface-related multiple reflections.
- 3a (optional). Estimation of θ and transformation to the natural coordinate system.
- 3b. Independent estimation of the P-wave and (slow and fast) S-wave macromodels.
4. Independent redatuming of the P-P, P-S, S-P and S-S data from the acquisition surface to the upper boundary of a target zone.

In the target zone the processing could be continued as follows:

5. Elastic stratigraphic inversion for the detailed elastic parameters $c_p(\mathbf{r})$, $c_s(\mathbf{r})$ and $\rho(\mathbf{r})$.
6. Lithological inversion for the rock and pore parameters.

Note that these last two steps require the redatumed P-P and S-S data as input (and to a smaller extent the redatumed P-S and S-P data). Of course this simultaneous inversion can only be successful when the different redatumed data sets are fully consistent. This demand is just as critical as the demand for the very accurate macromodel when omitting the decomposition process. Thus it may appear that nothing was gained by the decomposition process. However, the following two remarks can be made:

1. When structural information about the target zone is the main objective, then processing steps 1 to 4 give significantly better results than acoustic processing. (The target related P-/and S-events are well separated, which facilitates a much more reliable structural interpretation of the target zone).
2. When elastic (and lithological) information about the target zone is also required, then step(s) 5 (and 6) may be carried out after 'fine tuning' the different redatumed data sets. When the macromodels used in step 4 were not too much in error, then this fine tuning is simply a time shift in order to align the reflections from the top of the target zone in the different redatumed data sets. This time shift may be included as a parameter in the elastic stratigraphical inversion (step 5, De Haas 1992).

ELASTIC ONE-WAY WAVEFIELD EXTRAPOLATION OPERATORS

We now define forward and inverse elastic one-way wavefield extrapolation operators. The forward operators are the basis for a forward model of multicomponent

seismic data (next section). The inverse operators will be used in the discussion of the redatuming scheme.

In practical situations the wavefields are discretized along the x - and y -axes. Hence, the Rayleigh integrals may be rewritten in Berkhout's matrix notation. For forward extrapolation of downgoing P- and S-waves from depth level z_0 to z_t , we rewrite (5a) and (5c) as

$$\hat{\mathbf{p}}^+(z_t) = \hat{\mathbf{W}}^+(z_t, z_0)\hat{\mathbf{p}}^+(z_0) \quad (6a)$$

and for forward extrapolation of upgoing P- and S-waves, we write

$$\hat{\mathbf{p}}^-(z_0) = \hat{\mathbf{W}}^-(z_0, z_t)\hat{\mathbf{p}}^-(z_t), \quad (6b)$$

where

$$\hat{\mathbf{p}}^\pm = \begin{bmatrix} \phi^\pm \\ \hat{\psi}_x^\pm \\ \hat{\psi}_y^\pm \end{bmatrix} \quad (7a)$$

and

$$\hat{\mathbf{W}}^\pm = \begin{bmatrix} \mathbf{W}_{\phi, \phi}^\pm & \mathbf{0} & \mathbf{0} \\ \mathbf{0} & \hat{\mathbf{W}}_{\psi_x, \psi_x}^\pm & \mathbf{0} \\ \mathbf{0} & \mathbf{0} & \hat{\mathbf{W}}_{\psi_y, \psi_y}^\pm \end{bmatrix}. \quad (7b)$$

Vectors $\phi^\pm(z_0)$ and $\phi^\pm(z_t)$ contain one frequency component of the discretized versions of the wavefields $\phi^\pm(x, y, z_0; \omega)$ and $\phi^\pm(x, y, z_t; \omega)$ respectively. Similarly, vectors $\hat{\psi}_h^\pm(z_0)$ and $\hat{\psi}_h^\pm(z_t)$ contain one frequency component of the discretized versions of the wavefield $\hat{\psi}_h^\pm(x, y, z_0; \omega)$ and $\hat{\psi}_h^\pm(x, y, z_t; \omega)$ respectively, for $h = x$ or y . The extrapolation matrices $\mathbf{W}_{\phi, \phi}^\pm$ and $\hat{\mathbf{W}}_{\psi_h, \psi_h}^\pm$ contain discretized scaled versions of the z -derivatives of the Green's wavefields $\gamma_{\phi, \phi}^\pm$ and $\hat{\gamma}_{\psi_h, \psi_h}$ respectively (for more general expressions see Wapenaar and Berhout 1989, chapter VI). Note that these equations apply to an inhomogeneous, azimuthally anisotropic medium. The underlying assumptions are that the medium is locally homogeneous and isotropic at $z = z_0$ and $z = z_t$ and that the contrasts in the region $z_0 < z < z_t$ are weak to moderate (paper I).

For inverse extrapolation we write

$$\hat{\mathbf{p}}^+(z_0) = \hat{\mathbf{F}}^+(z_0, z_t)\hat{\mathbf{p}}^+(z_t) \quad (8a)$$

and

$$\hat{\mathbf{p}}^-(z_t) = \hat{\mathbf{F}}^-(z_t, z_0)\hat{\mathbf{p}}^-(z_0), \quad (8b)$$

where

$$\hat{\mathbf{F}}^\pm = \begin{bmatrix} \mathbf{F}_{\phi, \phi}^\pm & \mathbf{0} & \mathbf{0} \\ \mathbf{0} & \hat{\mathbf{F}}_{\psi_x, \psi_x}^\pm & \mathbf{0} \\ \mathbf{0} & \mathbf{0} & \hat{\mathbf{F}}_{\psi_y, \psi_y}^\pm \end{bmatrix}. \quad (8c)$$

Using the results from paper I, we find

$$\hat{\mathbf{F}}^+(z_0, z_t) = [\hat{\mathbf{W}}^-(z_0, z_t)]^* \tag{9a}$$

and

$$\hat{\mathbf{F}}^-(z_t, z_0) = [\hat{\mathbf{W}}^+(z_t, z_0)]^*, \tag{9b}$$

where * denotes complex conjugation.

FORWARD MODEL OF MULTICOMPONENT SEISMIC DATA

First we consider the response of an elastic subsurface bounded by a reflection-free surface at z_0 . With reference to Fig. 4 we write

$$\hat{\mathbf{p}}^-(z_0) = \hat{\mathbf{X}}(z_0, z_0)\hat{\mathbf{p}}^+(z_0), \tag{10a}$$

where

$$\hat{\mathbf{X}}(z_0, z_0) = \begin{bmatrix} \mathbf{X}_{\phi, \phi}(z_0, z_0) & \mathbf{X}_{\phi, \psi_x}(z_0, z_0) & \mathbf{X}_{\phi, \psi_y}(z_0, z_0) \\ \mathbf{X}_{\psi_x, \phi}(z_0, z_0) & \mathbf{X}_{\psi_x, \psi_x}(z_0, z_0) & \mathbf{X}_{\psi_x, \psi_y}(z_0, z_0) \\ \mathbf{X}_{\psi_y, \phi}(z_0, z_0) & \mathbf{X}_{\psi_y, \psi_x}(z_0, z_0) & \mathbf{X}_{\psi_y, \psi_y}(z_0, z_0) \end{bmatrix}, \tag{10b}$$

(see also Wapenaar *et al.* 1990, hereafter referred to as paper II.) The vector $\hat{\mathbf{p}}^+(z_0)$ contains one frequency component of a discretized downgoing elastic wavefield at z_0 in terms of P- and S-wave potentials, see (7a). This elastic wavefield propagates into the inhomogeneous anisotropic subsurface $z > z_0$, is partly reflected at the layer boundaries and propagates up to the surface. The monochromatic upgoing wavefield arriving at the surface is denoted by $\hat{\mathbf{p}}^-(z_0)$. According to equation (10a), the multicomponent one-way response matrix $\hat{\mathbf{X}}(z_0, z_0)$ describes the relationship between the downgoing and upgoing one-way wavefields at z_0 . Any of the submatrices in (10b) represents a single-component one-way response of the elastic subsurface. For example, matrix $\mathbf{X}_{\phi, \psi_y}(z_0, z_0)$ describes the relationship between downgoing S_y -waves and upgoing P-waves at z_0 .

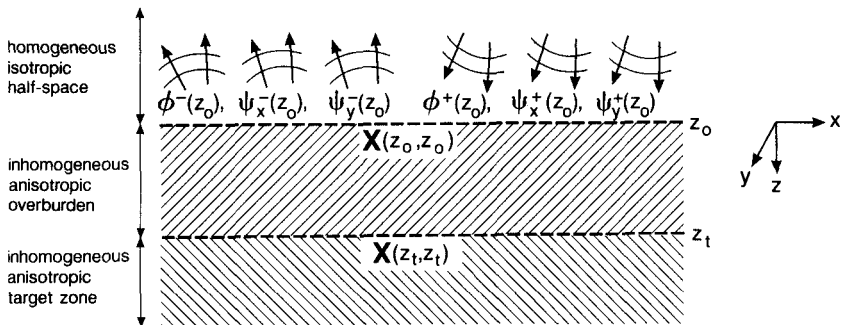


FIG. 4. The one-way response matrix $\mathbf{X}(z_0, z_0)$ describes the relationship between downgoing and upgoing wavefields at acquisition depth level z_0 . The one-way response matrix $\mathbf{X}(z_t, z_t)$ describes the relationship between downgoing and upgoing wavefields at target depth level z_t .

One column of the matrix contains the upgoing P-waves at z_0 due to a downgoing S_y -wave at one lateral position at z_0 . Hence, this column may also be interpreted as one frequency component of a 'common shot record' for one S_y -wave source and many P-wave receivers at z_0 (see paper II, Appendix A).

In the following, in the subsurface $z > z_0$ we distinguish between an overburden $z_0 < z < z_t$ and a target zone $z > z_t$ (Fig. 4). For the one-way response of the target zone we write, in analogy with (10a),

$$\hat{\mathbf{p}}^-(z_t) = \hat{\mathbf{X}}(z_t, z_0)\hat{\mathbf{p}}^+(z_0). \tag{11}$$

Substituting (6a) and (6b) yields

$$\hat{\mathbf{p}}^-(z_0) = \hat{\mathbf{W}}^-(z_0, z_t)\hat{\mathbf{X}}(z_t, z_0)\hat{\mathbf{W}}^+(z_t, z_0)\hat{\mathbf{p}}^+(z_0). \tag{12}$$

Comparing this expression with (10a) yields

$$\hat{\mathbf{X}}(z_0, z_0) = \hat{\mathbf{W}}^-(z_0, z_t)\hat{\mathbf{X}}(z_t, z_0)\hat{\mathbf{W}}^+(z_t, z_0) \tag{13}$$

(see Fig. 5). Equation (13) describes the relationship between the response matrix at a reflection-free acquisition surface and the response matrix at the upper boundary of the target zone. Note that mode conversion during propagation is neglected [see (7b)]. However, mode conversion during reflection is included (see (10b) with z_0 replaced by z_t). Also note that the response of the overburden is ignored. Equation (13) will serve as the basis for the redatuming scheme, discussed in the next section.

In general, the natural coordinate system of the anisotropic medium does not correspond with the acquisition coordinate system. Hence, before relating $\hat{\mathbf{X}}(z_0, z_0)$ to the acquisition parameters, we define a coordinate transformation, according to

$$\mathbf{X}(z_0, z_0) = \mathbf{\Theta}^T(z_0)\hat{\mathbf{X}}(z_0, z_0)\mathbf{\Theta}(z_0), \tag{14a}$$

with

$$\mathbf{\Theta}(z_0) = \begin{bmatrix} \mathbf{I} & \mathbf{0} & \mathbf{0} \\ \mathbf{0} & \mathbf{I} \cos \theta & \mathbf{I} \sin \theta \\ \mathbf{0} & -\mathbf{I} \sin \theta & \mathbf{I} \cos \theta \end{bmatrix} \tag{14b}$$

(Alford 1986), where θ is the angle between the two coordinate systems.

In practical situations, the surface z_0 represents the earth's free surface which is a perfect reflector for the upgoing waves $\mathbf{p}^-(z_0)$. In paper II we showed that multiple

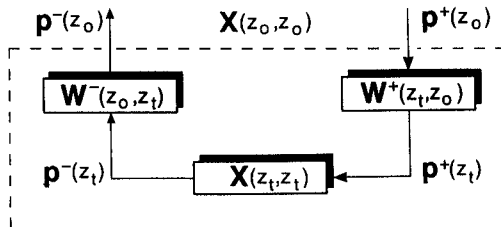


FIG. 5. The one-way response matrices $\mathbf{X}(z_0, z_0)$ and $\mathbf{X}(z_t, z_t)$ are related via the one-way extrapolation matrices $\mathbf{W}^+(z_t, z_0)$ and $\mathbf{W}^-(z_0, z_t)$.

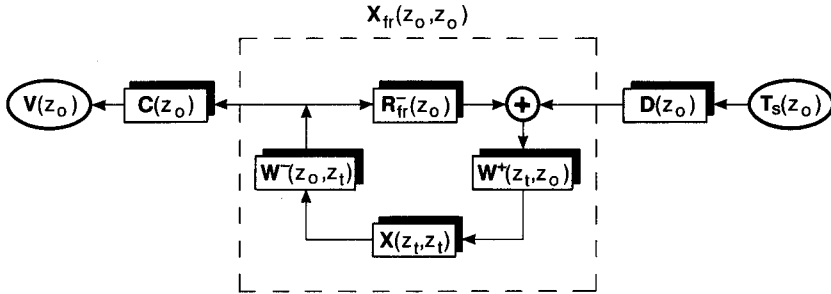


FIG. 6. Forward model for multicomponent seismic data (the surface waves and the response of the overburden are ignored).

reflections related to the free surface can be included, according to

$$\mathbf{X}_{fr}(z_0, z_0) = [\mathbf{I} - \mathbf{X}(z_0, z_0)\mathbf{R}_{fr}^-(z_0)]^{-1}\mathbf{X}(z_0, z_0), \tag{15a}$$

where $\mathbf{R}_{fr}^-(z_0)$ describes the reflectivity of the free surface for the upgoing waves $\mathbf{p}^-(z_0)$ and where $\mathbf{X}_{fr}(z_0, z_0)$ is the one-way response matrix at the free surface. In paper II we also derived the following relationship between the one-way response matrix $\mathbf{X}_{fr}(z_0, z_0)$ and the two-way seismic data:

$$\mathbf{V}(z_0) = \mathbf{C}(z_0)\mathbf{X}_{fr}(z_0, z_0)\mathbf{D}(z_0)\mathbf{T}_s(z_0). \tag{15b}$$

From right to left (15b) contains a source matrix $\mathbf{T}_s(z_0)$ (each column containing the traction of a seismic vibrator at the free surface), a decomposition matrix $\mathbf{D}(z_0)$ (transforming the tractions into downgoing P- and S-waves), the one-way response matrix $\mathbf{X}_{fr}(z_0, z_0)$ (describing the response of the subsurface, including the multiple reflections related to the free surface), and a composition matrix $\mathbf{C}(z_0)$ (transforming the upgoing P- and S-waves into the particle velocities $\mathbf{V}(z_0)$ at the free surface). The forward model, described by (13), (14) and (15) is visualized in Fig. 6. Note that this forward model is not a proposal for a numerical modelling scheme for multicomponent seismic data. The only purpose of this section was to provide a starting point of a systematic discussion of the elastic redatuming scheme.

ELASTIC REDATUMING OF MULTICOMPONENT SEISMIC DATA

Given the forward model, described by (13), (14) and (15), elastic redatuming of Fourier transformed multicomponent seismic data involves, for each frequency component, the following steps:

- 1 Decomposition of the multicomponent data [matrix $\mathbf{V}(z_0)$] into P-P, P-S, S-P and S-S data [matrix $\mathbf{X}_{fr}(z_0, z_0)$]. This is accomplished by inverting (15b), see paper II.
2. Elimination of the surface-related multiple reflections. This is accomplished by inverting (15a), yielding the one-way response matrix $\mathbf{X}(z_0, z_0)$, see paper II.
- 3a. (optional). Estimation of the azimuth angle θ (Alford 1986) and inversion of (14), yielding the one-way response matrix $\hat{\mathbf{X}}(z_0, z_0)$, defined in the natural coordinate system of the azimuthally anisotropic medium.

- 3b. Independent estimation of the P-wave macromodel from the travelttime information contained in submatrix $\mathbf{X}_{\phi, \phi}(z_0, z_0)$ and the (slow and fast) S-wave macromodels from submatrices $\hat{\mathbf{X}}_{\psi_x, \psi_x}(z_0, z_0)$ and $\hat{\mathbf{X}}_{\psi_y, \psi_y}(z_0, z_0)$. Independent estimation of the P-wave and S-wave macromodels is equivalent to acoustic macromodel estimation as described by Faye and Jeannot (1986) and Cox *et al.* (1988).
4. Independent redatuming of the P-P, P-S, S-P and S-S data from the acquisition surface z_0 to the upper boundary z_t of a target zone. This is accomplished by inverting (13), yielding the one-way response matrix $\hat{\mathbf{X}}(z_t, z_t)$.

We now proceed with the inversion of (13). Upon substitution of (7b) and (10b) into (13) we obtain nine independent expressions of the single-component one-way response submatrices. They may be summarized as

$$\hat{\mathbf{X}}_{\beta, \alpha}(z_0, z_0) = \hat{\mathbf{W}}_{\beta, \beta}^-(z_0, z_t) \hat{\mathbf{X}}_{\beta, \alpha}(z_t, z_t) \hat{\mathbf{W}}_{\alpha, \alpha}^+(z_t, z_0), \quad (16)$$

where α and β may stand for ϕ or ψ_x or ψ_y . Note that these equations are independent because we neglected mode conversion during propagation through the overburden [see (6) and (7)]. Hence inverting (13) is equivalent to inverting (16) *independently* for the nine submatrices $\hat{\mathbf{X}}_{\beta, \alpha}(z_t, z_t)$:

$$\hat{\mathbf{X}}_{\beta, \alpha}(z_t, z_t) = [\hat{\mathbf{W}}_{\beta, \beta}^-(z_0, z_t)]^{-1} \hat{\mathbf{X}}_{\beta, \alpha}(z_0, z_0) [\hat{\mathbf{W}}_{\alpha, \alpha}^+(z_t, z_0)]^{-1}, \quad (17a)$$

or

$$\hat{\mathbf{X}}_{\beta, \alpha}(z_t, z_t) = \hat{\mathbf{F}}_{\beta, \beta}^-(z_t, z_0) \hat{\mathbf{X}}_{\beta, \alpha}(z_0, z_0) \hat{\mathbf{F}}_{\alpha, \alpha}^+(z_0, z_t), \quad (17b)$$

where the inverse extrapolation operators $\hat{\mathbf{F}}_{\alpha, \alpha}^+(z_0, z_t)$ and $\hat{\mathbf{F}}_{\beta, \beta}^-(z_t, z_0)$ are given in (8) and (9). Again, for simplicity the response of the overburden is ignored. In reality $\hat{\mathbf{X}}_{\beta, \alpha}(z_t, z_t)$, as defined by (17), consists of a causal term representing the target response and a non-causal term related to the overburden response. The latter can be removed after the redatumed data have been transformed back to the time domain.

Note that elastic redatuming of decomposed data as described by (17b) is very similar to acoustic redatuming as described by Berkhout (1985). Note that (17b) could be written as a two-step procedure, according to

$$\hat{\mathbf{X}}_{\beta, \alpha}(z_t, z_0) = \hat{\mathbf{F}}_{\beta, \beta}^-(z_t, z_0) \hat{\mathbf{X}}_{\beta, \alpha}(z_0, z_0), \quad (18a)$$

followed by

$$\hat{\mathbf{X}}_{\beta, \alpha}(z_t, z_t) = \hat{\mathbf{X}}_{\beta, \alpha}(z_t, z_0) \hat{\mathbf{F}}_{\alpha, \alpha}^+(z_0, z_t) \quad (18b)$$

(see also Fig. 7). Equation (18a) describes a lateral deconvolution process along the receivers in each 'common shot record' [i.e., along the columns of $\hat{\mathbf{X}}_{\beta, \alpha}(z_0, z_0)$]. Physically it means that the receivers are downward extrapolated from the acquisition surface z_0 to the target depth level z_t . Hence, $\hat{\mathbf{X}}_{\beta, \alpha}(z_t, z_0)$ represents the one-way target response in terms of upgoing β -waves at z_t , related to downgoing α -waves at z_0 . Equation (18b) describes a lateral deconvolution process along the sources in each common receiver record [i.e. along the rows of $\hat{\mathbf{X}}_{\beta, \alpha}(z_t, z_0)$]. Physically it

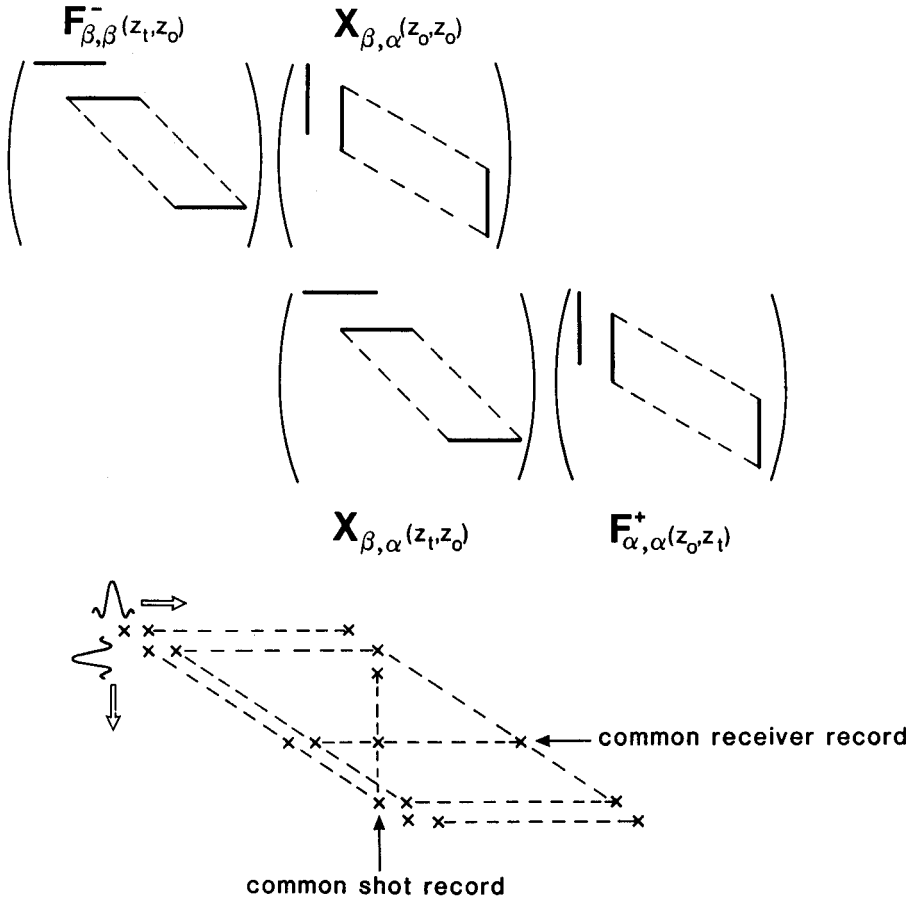


FIG. 7. According to (18), elastic redatuming involves lateral deconvolution processes along the receivers in each common shot record and along the sources in each common receiver record.

means that the sources are downward extrapolated from z_0 to z_t . Note that the acoustic redatuming scheme described by Berryhill (1984) is based on a similar principle. For practical applications, redatuming according to (18a) and (18b) may not be the most efficient solution. Particularly for 3D applications it involves a cumbersome data reordering process (from common shot records into common receiver records) in between the two steps. Berkhout (1985) and Wapenaar and Berkhout (1987) show that (18a) and (18b) can be rewritten as redatuming per shot record, followed by 'stacking', without loss of accuracy.

EXAMPLE OF ELASTIC REDATUMING

We illustrate the elastic redatuming procedure with a 2D example. For the isotropic subsurface configuration of Fig. 8, we generated 128 multicomponent

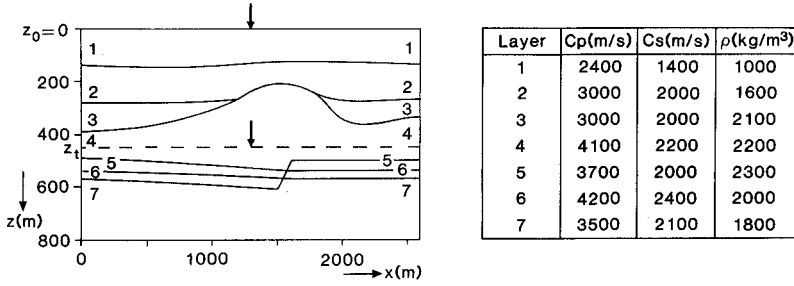


FIG. 8. 2D inhomogeneous elastic subsurface. The multicomponent vibrators and geophones are situated at the free surface $z_0 = 0$ m.

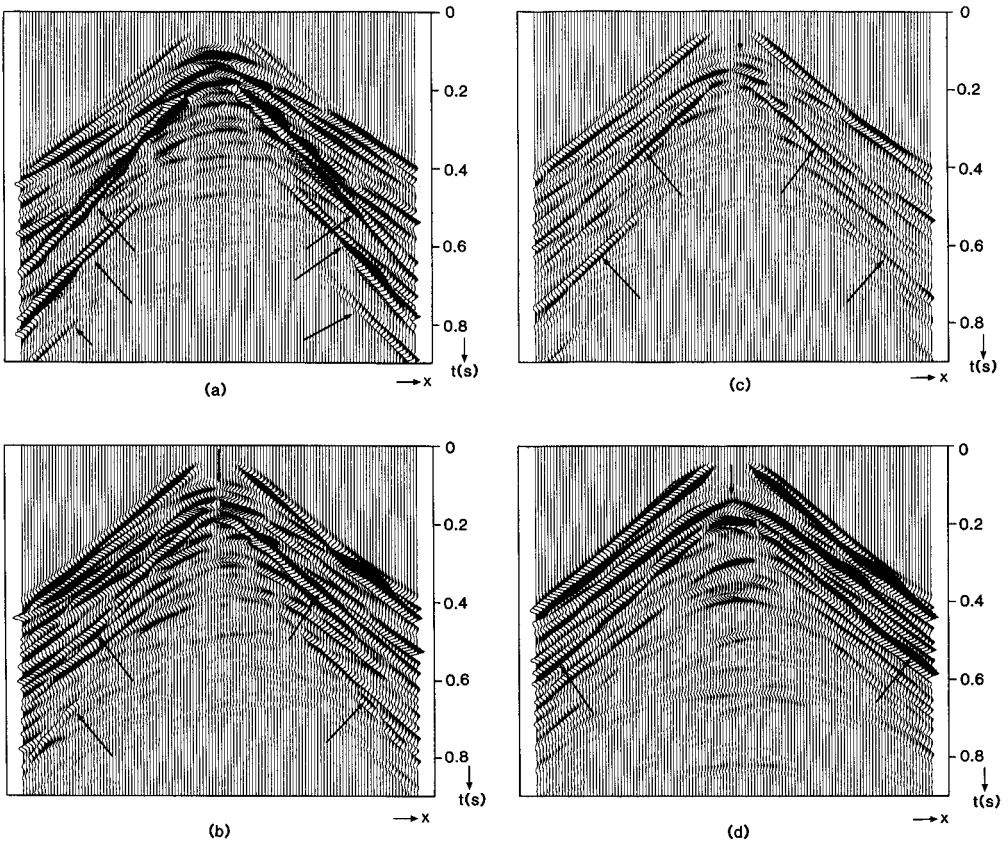


FIG. 9. Multicomponent shot record. The source position is indicated by the arrow in Fig. 8. (a) Pseudo P-P data; (b) Pseudo SV-P data; (c) Pseudo P-SV data; (d) Pseudo SV-SV data.

seismic shot records by finite-difference modelling (Kelly *et al.* 1976; Haimé 1987). We used vertical and horizontal vibrators as well as vertical and horizontal geophones at the free surface z_0 . One multicomponent shot record is shown in the space-time domain in Fig. 9. Following the procedure described in paper II, we decomposed these data into true P-P, SV-P, P-SV and SV-SV responses and we eliminated the multiple reflections related to the free surface (in the 2D situation S_y -waves are equivalent to SV-waves). The result is shown in Fig. 10. Note that, unlike in Fig. 9, the response of the target reflectors below $z_t = 450$ m can be clearly recognized. Following the procedure described by Cox *et al.* (1988), we estimated the overburden P-wave macromodel from the P-P data (Fig. 10a) and the S-wave macromodel from the SV-SV data (Fig. 10d). The results are shown in Fig. 11. Note that the estimated P-wave macromodel (Fig. 11a) is quite accurate (errors less than 4%, except in the third thin layer). The estimated S-wave macromodel (Fig. 11b) is

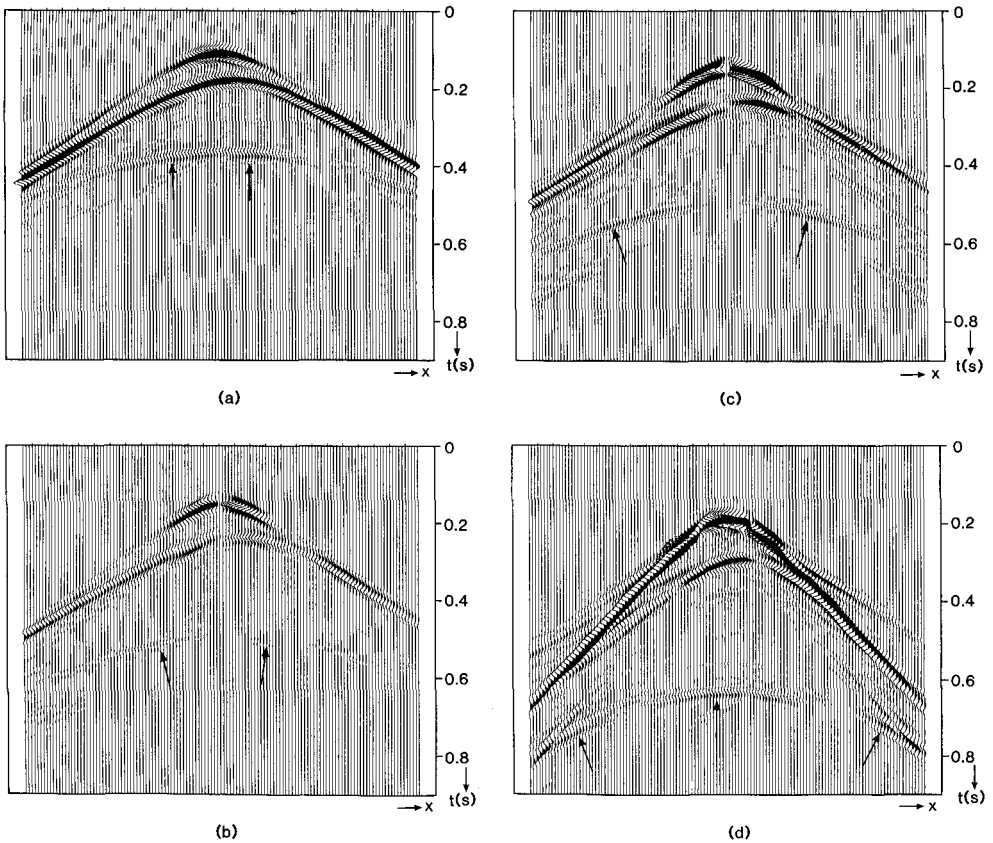


FIG. 10. Multicomponent shot record, after elastic decomposition and multiple elimination. The source position is indicated by the arrow in Fig. 8. (a) True P-P data; (b) true SV-P data; (c) True P-SV data; (d) true SV-SV data. The arrows indicate the response of the target reflectors below $z_t = 450$ m.

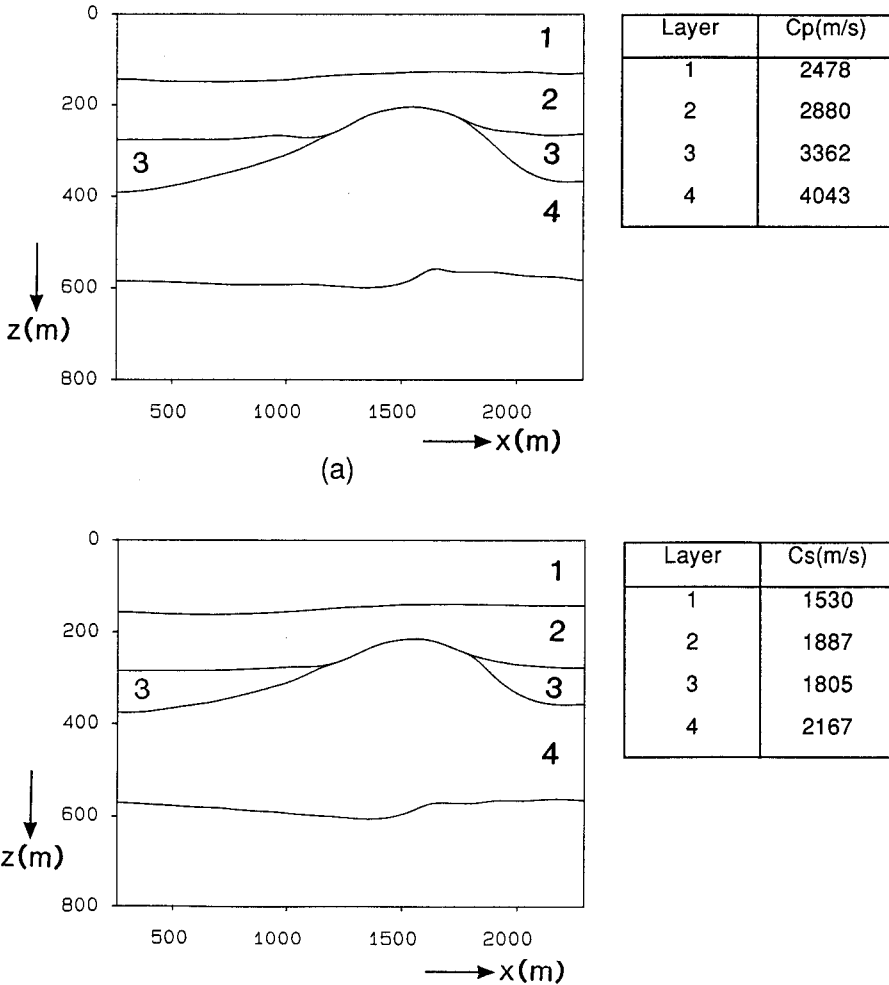


FIG. 11. (a) P-wave macromodel, estimated from the P-P data (Fig. 10a); (b) S-wave macromodel, estimated from the SV-SV data (Fig. 10d).

less accurate. This is explained by the significant angle-dependent behaviour of the SV-SV reflections.

We now come to the actual redatuming procedure. Transforming the data of Figs. 10a, b, c, d from the time domain to the frequency domain yields for each frequency in the seismic band ($5 \text{ Hz} < f = \omega/(2\pi) < 80 \text{ Hz}$) one column of the matrices $\mathbf{X}_{\phi, \phi}(z_0, z_0)$, $\mathbf{X}_{\psi_y, \phi}(z_0, z_0)$, $\mathbf{X}_{\phi, \psi_y}(z_0, z_0)$ and $\mathbf{X}_{\psi_y, \psi_y}(z_0, z_0)$, respectively. The full matrices are obtained by repeating this procedure for all 128 decomposed multi-component shot records in the seismic line.

Elastic redatuming now involves applying (17) or (18) for $\alpha = \phi, \psi_y$, and $\beta = \phi, \psi_y$ for each frequency in the seismic band. The columns of the resulting matrices $\mathbf{X}_{\phi, \phi}(z_1, z_1)$, $\mathbf{X}_{\psi_y, \phi}(z_1, z_1)$, $\mathbf{X}_{\phi, \psi_y}(z_1, z_1)$ and $\mathbf{X}_{\psi_y, \psi_y}(z_1, z_1)$ contain the (monochromatic)

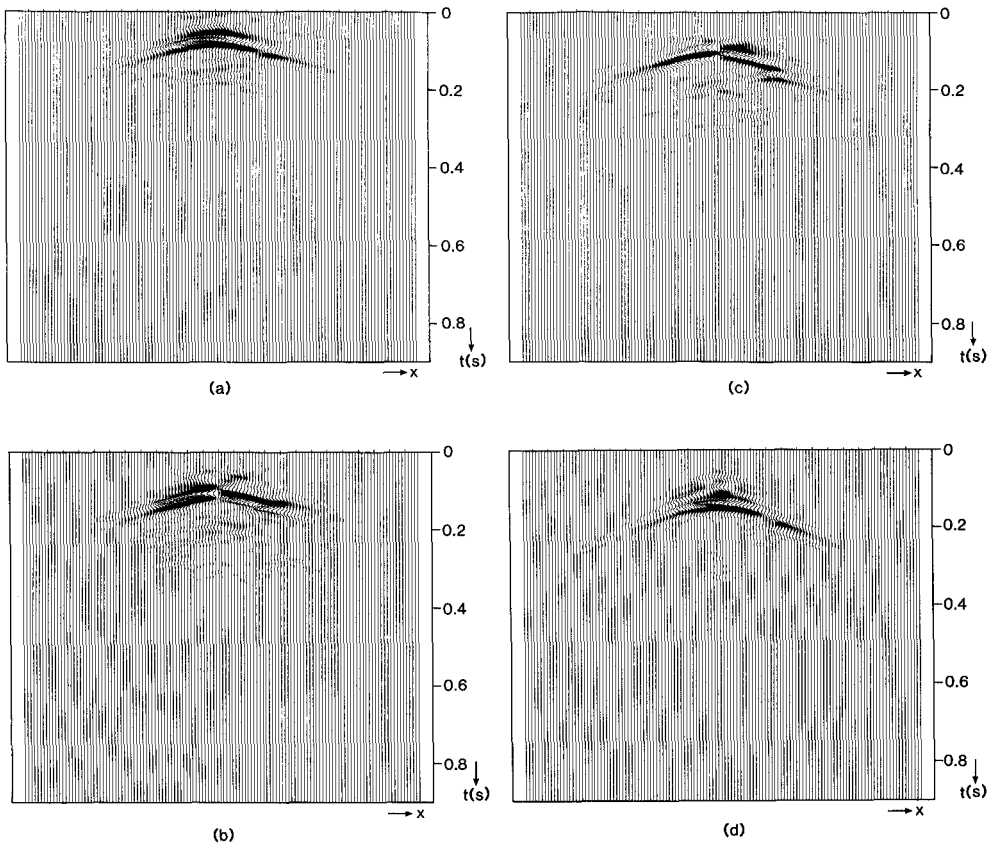


FIG. 12. Multicomponent shot record, selected from the elastically redatumed data at z_t . The source position is indicated by the arrow at $z_t = 450$ m in Fig. 8. (a) True P-P data; (b) true SV-P data; (c) true P-SV data; (d) true SV-SV data.

shot records at the upper boundary z_t of the target zone. Next, these results are transformed back to the time domain. Figure 12 shows one multicomponent shot record after redatuming. Note that this result clearly shows the angle-dependent reflectivity properties of the reflectors in the target. Figure 13 shows the P-P and SV-SV zero-offset sections, selected from the redatumed data at the upper boundary of the target zone. Note that the structure of the reflectors in the target can be clearly recognized. Comparison of the redatuming results (Fig. 12 and 13) with the input data (Fig. 9) shows that the total processing sequence considerably reduced the complexity of the target reflections.

CONCLUSIONS

In principle, elastic redatuming may be carried out before or after decomposition of the multicomponent data into independent P-P, P-S, S-P and S-S responses. From a theoretical point of view, both approaches are equivalent. However, from a practical

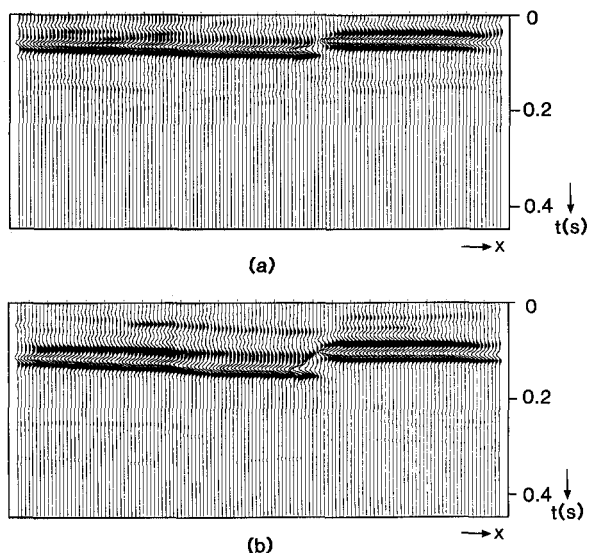


FIG. 13. Zero-offset sections, selected from the elastically redatumed data at z_1 . (a) True P-P data; (b) true SV-SV data.

point of view redatuming before decomposition is unattractive because the quality of the results depends heavily on the consistency of the P- and S-wave macromodels.

Decomposition at the surface of the multicomponent data enables independent estimation of the P- and S-wave macromodels as well as independent redatuming of the P-P, P-S, S-P and S-S data from the acquisition surface to the upper boundary of the target zone. After decomposition, the requirements for the accuracy of the P- and S-wave macromodels are not more rigorous than in the acoustic situation.

We have shown that elastic redatuming of decomposed data can be elegantly written in terms of matrix multiplications (17), analogously to acoustic redatuming (Berkhout 1985). After redatuming, the propagation effects (down and up) of the target overburden have been removed from the target reflections and, particularly for a structurally complicated overburden, the target response will be simplified significantly.

REFERENCES

- AKI, K. and RICHARDS, P.G. 1980. *Quantitative Seismology*. W.H. Freeman & Co.
- ALFORD, R.M. 1986. Shear data in the presence of azimuthal anisotropy: Dilley, Texas. *56th SEG meeting, Houston, Expanded Abstracts*, 476-479.
- BERKHOUT, A.J. 1985. *Seismic Migration: Imaging of Acoustic Energy by Wave-field Extrapolation. A. Theoretical Aspects*. Elsevier Science Publishing Co.
- BERKHOUT, A.J. 1986. Seismic inversion in terms of prestack migration and multiple elimination. *Proceedings of the IEEE* **74**, 415-427.
- BERKHOUT, A.J. and WAPENAAR, C.P.A. 1988. Delft philosophy on inversion of elastic data. *58th SEG meeting, Anaheim, Expanded Abstracts*, 831-833.

- BERRYHILL, J.R. 1984. Wave equation datuming before stack. *Geophysics* **49**, 2064–2066.
- BURRIDGE, R. and KNOPOFF, L. 1964. Body force equivalents for seismic dislocations. *Bulletin of the Seismological Society of America* **54**, 1875–1888.
- COX, H.L.H., OOMS, F.P.J., WAPENAAR, C.P.A. and BERKHOUT, A.J. 1988. Verification of macro subsurface models using a shot record approach. *58th SEG meeting, Anaheim, Expanded Abstracts*, 904–908.
- DE HAAS, J.C. 1992. *Elastic stratigraphic inversion, an integrated approach*. D.Sc. thesis, Delft University of Technology.
- DE HOOP, A.T. 1958. *Representation theorems for the displacement in an elastic solid and their application to elastodynamic diffraction theory*. D.Sc. thesis, Delft University of Technology.
- FAYE, J.P. and JEANNOT, J.P. 1986. Pre-stack migration velocities from focusing depth analysis. *56th SEG meeting, Houston, Expanded Abstracts*, 438–440.
- HAIMÉ, G.C. 1987. *Full elastic inverse wave field extrapolation through an inhomogeneous medium*. M.Sc. thesis, Delft University of Technology.
- KELLY, K.R., WARD, R.W., TREITEL, S. and ALFORD, R.M. 1976. Synthetic seismograms: a finite-difference approach. *Geophysics* **41**, 2–27.
- KINNEGING, N.A., BUDEJICKY, V., WAPENAAR, C.P.A. and BERKHOUT, A.J. 1989. Efficient 2D and 3D shot record redatuming. *Geophysical Prospecting* **37**, 493–530.
- WAPENAAR, C.P.A. and BERKHOUT, A.J. 1987. Full prestack versus shot record migration. *57th SEG meeting, New Orleans, Expanded Abstracts*, 761–764.
- WAPENAAR, C.P.A. and BERKHOUT, A.J. 1989. *Elastic Wavefield Extrapolation: Redatuming of Single- and Multicomponent Seismic Data*. Elsevier Science Publishing Co.
- WAPENAAR, C.P.A. and HAIMÉ, G.C. 1990. Elastic extrapolation of primary seismic P- and S-waves. *Geophysical Prospecting* **38**, 23–60 (paper I in text).
- WAPENAAR, C.P.A., HERRMANN, P., VERSCHUUR, D.J. and BERKHOUT, A.J. 1990. Decomposition of multicomponent seismic data into primary P- and S-wave responses. *Geophysical Prospecting* **38**, 633–661 (paper II in text).